second-order perturbation theory allowing for off-diagonal Hamiltonian terms, and the other of which is due to the change in the dispersion relation. The contribution from the off-diagonal terms is given by the expression

$$E_{\rm gr}^{a,\,\rm ellipt} = 8t^2\,\frac{|\Delta_1|^2\,|\Delta_2|^2}{\Delta^4} \times \sum_{\mathbf{p}} \frac{(\cos^2 p_x + \cos^2 p_y)\,\Delta^2}{\left[\Delta^2 + 16(t')^2\cos^2 p_x \cos^2 p_y\right]^{3/2}} + \ldots, \quad (24)$$

where, as before, the ellipsis refers to the terms that depend only on Δ. The contribution due to the change in the dispersion of the diagonal Hamiltonian terms is written out as follows:

$$E_{\rm gr}^{b,\,\rm ellipt} = -8t^2\,\frac{|\Delta_1|^2\,|\Delta_2|^2}{\Delta^4} \times \sum_{\mathbf{p}} \frac{(\cos^2 p_x + \cos^2 p_y)\,\Delta^2}{\left[\Delta^2 + 16(t')^2\cos^2 p_x \cos^2 p_y\right]^{3/2}} + \ldots. \quad (25)$$

Comparing Eqns (25) and (24), we see that the two contributions cancel out. Thus, including elliptical electron pockets into the $t-t'-U$ model does not lift the degeneracy of the SDW order parameter. This result will most likely be true if the higher-order terms in the expansion of the energy in a power series of t/t' are included.

In this talk, the formation mechanism of spin density waves in iron-based pnictides were analyzed based on the results of paper [16]. We have considered a model of itinerant electrons with two hole Fermi surfaces centered around the Γ point of the Brillouin iron zone and with two electron pockets near $(0,\pi)$ and $(\pi,0)$ points.

In general, the SDW order parameter in this model is a combination of two components with respective wave vectors $\mathbf{Q}_2$ $(0,\pi)$ and $\mathbf{Q}_1$ $(\pi,0)$. However, only one of these components is observed in neutron scattering experiments. As shown in the talk, indeed only one of the components, $(0,\pi)$ or $(\pi,0)$, is stabilized if only one of the hole bands is assumed to mix with the electron bands when SDW states form. The other hole band remains gapless, which is precisely what explains the metallicity of pnictides with SDWs. For perfect nesting, the SDW order parameter in this three-band model is strongly degenerate. This degeneracy is lifted in favor of either $(0,\pi)$ ordering or $(\pi,0)$ ordering by including interactions and elliptical electron pockets. The calculated Fermi contours, ARPES spectral intensity, and the band dispersion near the Fermi level are consistent with the experimental data.

Acknowledgments

I would like thank I I Mazin and A V Chubukov for valuable comments. The work was supported by the Russian Federation Government Program of Competitive Growth of Kazan (Volga region) Federal University.

References

1. Kamihara Y et al. *J. Am. Chem. Soc.* **130** 3296 (2008)
2. Hirschfeld P J, Korshunov M M, Mazin I I *Rep. Prog. Phys.* **74** 124508 (2011)
3. Liu C et al. *Phys. Rev. Lett.* **101** 177005 (2008)
4. Terashima K et al. *Proc. Natl. Acad. Sci. USA* **106** 7330 (2009)
5. Zabolotnyy V B et al. *Nature* **457** 569 (2009)
6. Yang L X et al. *Phys. Rev. Lett.* **102** 107002 (2009)
7. Lu D H et al. *Nature* **455** 81 (2008)
8. Ding H et al. *J. Phys. Condens. Matter* **23** 135701 (2011)
9. Richard P et al. *Rep. Prog. Phys.* **74** 124512 (2011)
10. Coldea A I et al. *Phys. Rev. Lett.* **101** 216402 (2008)
11. Shishido H et al. *Phys. Rev. Lett.* **104** 057008 (2010)
12. Carrington A *Rep. Prog. Phys.* **74** 124507 (2011)
13. Singh D J, Du M-H *Phys. Rev. Lett.* **100** 237003 (2008)
14. Boeri L, Dolgov O V, Golubov A A *Phys. Rev. Lett.* **101** 026403 (2008)
15. Fernandes R M et al. *Phys. Rev. B* **85** 024534 (2012)
16. Eremin I, Chubukov A V *Phys. Rev. B* **81** 024511 (2010)
17. Chandra P, Coleman P, Larkin A I *Phys. Rev. Lett.* **64** 88 (1990)
18. Si Q, Abrahams E *Phys. Rev. Lett.* **101** 076401 (2008)
19. Xu C, Müller M, Sachdev S *Phys. Rev. B* **78** 020501(R) (2008)
20. Yildirim T *Phys. Rev. Lett.* **101** 057010 (2008)
21. Uhrig G S et al. *Phys. Rev. B* **79** 092416 (2009)
22. Nakajima M et al. *Phys. Rev. B* **81** 104528 (2010)
23. Rice T M *Phys. Rev. B* **2** 3619 (1970)
24. Keldysh L V, Kopaev Yu V *Sov. Phys. Solid State* **6** 2219 (1965); *Fiz. Tverd. Tela* **6** 2791 (1964)
25. Andersen O K, Boeri L *Ann. Physik* **523** 8 (2011)
26. Liu C et al. *Nature Phys.* **6** 419 (2010)
27. Pratt D K et al. *Phys. Rev. Lett.* **106** 257001 (2011)
28. Cvetkovic V, Tesanovic Z *Europhys. Lett.* **85** 37002 (2009)
29. Chubukov A V, Efremov D V, Eremin I *Phys. Rev. B* **78** 134512 (2008)
30. Brydon P M R, Timm C *Phys. Rev. B* **80** 174401 (2009)
31. Brydon P M R, Timm C *Phys. Rev. B* **79** 180504(R) (2009)
32. Wang F et al. *Phys. Rev. Lett.* **102** 047005 (2009)
33. Platt C, Honerkamp C, Hanke W *New J. Phys.* **11** 055058 (2009)
34. de la Cruz C et al. *Nature* **453** 899 (2008)
35. Klauss H-H et al. *Phys. Rev. Lett.* **101** 077005 (2008)
36. Fisher I R, Degiorgi L, Shen Z X *Rep. Prog. Phys.* **74** 124506 (2011)

PACS numbers: 74.20.Rp, **74.25.–q**, 74.62.Dh
DOI: 10.3367/UFNe.0184.201408h.0882

Superconducting state in iron-based materials and spin-fluctuation pairing theory

M M Korshunov

> *Beyond the pairs of opposites of which the world consists, other, new insights begin.*
> *Herman Hesse, "Inside and Outside,"* in *Stories of Five Decades* (London: Jonathan Cape, 1974)

Quite recently, the scientific community was shaken up by a new discovery. In the field of high-$T_{\rm c}$ superconductivity, where cuprates had overwhelmingly predominated for the previous two decades, a new player — iron compounds — has appeared [1]. Although the superconducting transition temperature ($T_{\rm c}$) in iron-based compounds has not exceeded the liquid-nitrogen temperature, already in late 2008, i.e., less than a year after the discovery of this new class of super-

M M Korshunov. Kirenskii Institute of Physics, Siberian Branch of the Russian Academy of Sciences, Krasnoyarsk, Russian Federation
E-mail: mkor@iph.krasn.ru

Uspekhi Fizicheskikh Nauk **184** (8) 882 – 888 (2014)
DOI: 10.3367/UFNr.0184.201408h.0882
Translated by S N Gorin; edited by A Radzig

conducting materials, this temperature reached 56 K. To date, the record among single crystals has belonged to $SmFeAsO_{1-x}F_x$ ($T_c = 57.5$ K) [2]; great hopes have been laid upon the discovery of superconductivity with $T_c \sim 60$ K in single-layer FeSe films [3, 4].

In general, superconducting iron materials can be grouped in two classes: pnictides, and chalcogenides. The basic element in these compounds is a square lattice of iron atoms, which in the majority of weakly doped compounds is subjected to orthorhombic distortions at temperatures comparable with the temperature of the transition to the antiferromagnetic (AFM) phase, T_{SDW}. In compounds of the first class, iron resides in a tetrahedral surrounding of arsenic or phosphorus atoms; in compounds of the second class, of selenium, tellurium, or sulfur atoms. The pnictides can be single-layer, e.g., 1111 compounds such as LaFeAsO, LaFePO, and Sr_2VO_3FeAs; and two-layer, such as 122, with two layers of FeAs per unit cell, e.g., $BaFe_2As_2$, KFe_2As_2. The chalcogenides include compounds of the 11 type ($Fe_{1-\delta}Se$, $Fe_{1+y}Te_{1-x}Se_x$, FeSe films). The structure and physical properties of iron compounds have been discussed in detail in many reviews (see, e.g., Refs [5–16]).

A characteristic feature of iron compounds as opposed to, for instance, cuprates, consists in a qualitative, or sometimes even quantitative, agreement of their Fermi surface (measured by the angle-resolved photoemission spectroscopy (ARPES) method and by the quantum oscillations method) with the Fermi surface calculated from the first principles. This peculiarity, together with the small magnitude of the magnetic moment in iron atoms ($\sim 0.3\mu_B$) in the pnictides and the absence of the dielectric state in the undoped case, make it possible to speak of a small or moderate level of electron correlations. Therefore, the natural starting point for their description is the model of itinerant electrons rather than the Mott–Hubbard limit and $t-J_1-J_2$ type models.

Soon after the discovery of superconductivity in pnictides, estimates were made of the possibility of pairing due to the electron–phonon interaction. The coupling constant appears to be even smaller than that for aluminum [17], although T_c in iron compounds is significantly higher. This led to the conclusion that it is unlikely that the pairing caused by electron–phonon interaction could play a leading role in the emergence of superconductivity, although a more thorough analysis is probably required to take into account some specific features of the electron band structure [18]. Such a situation immediately led to searching for alternative theories of superconducting pairing. The interactions that are analyzed in the theories vary from spin and orbital fluctuations to strongly correlated Mott–Hubbard and Hund's exchange constants. It is unrealistic to describe or even simply mention all these theories in the present paper; therefore, we focus on one of the most promising theories, namely, the spin–fluctuation theory of the superconducting pairing.

The spin–fluctuation theory of superconductivity is promising for a number of reasons: (1) this theory is based on the model of itinerant electrons, which serves as a good starting point for the description of iron compounds; (2) the superconducting phase arises directly after the AFM phase or coexists with it; in this case, the character of the spin–lattice relaxation rate $1/T_1T$ gradually changes from the Curie–Weiss to Pauli behaviors with an increase of doping and decreasing T_c [19], which indicates a decrease in the role of spin fluctuations; (3) the description of various experimentally observed properties of the pnictides and chalcogenides does not require the introduction of additional parameters into the theory; rather, only some specific features of the band structure and of the interactions in different classes of the iron compounds should be taken into account [16].

Iron-based superconductors represent quasi-two-dimensional substances in which the square lattice of iron atoms serves as the conducting plane. As was shown by the early calculations in the density functional theory (DFT) [20–22], which satisfactorily agree with the results of ARPES and quantum-oscillation measurements, it is the $3d^6$ states of Fe^{2+} that are dominant near the Fermi level. In this case, all five orbitals ($d_{x^2-y^2}$, $d_{3z^2-r^2}$, d_{xy}, d_{xz} and d_{yz}) lie on or near the Fermi surface. This leads to the substantial multiorbital and multiband character of the low-energy electron structure, which cannot be described already in a one-band model. Thus, for example, in the five-orbital model given in Ref. [23], which satisfactorily describes the results of DFT calculations [24], the Fermi surface consists of four pockets: two hole pockets near the (0, 0) point and two electron pockets in the vicinity of the $(\pi, 0)$ and $(0, \pi)$ points (Fig. 1). This geometry in the **k** space leads to the possibility of generating the spin

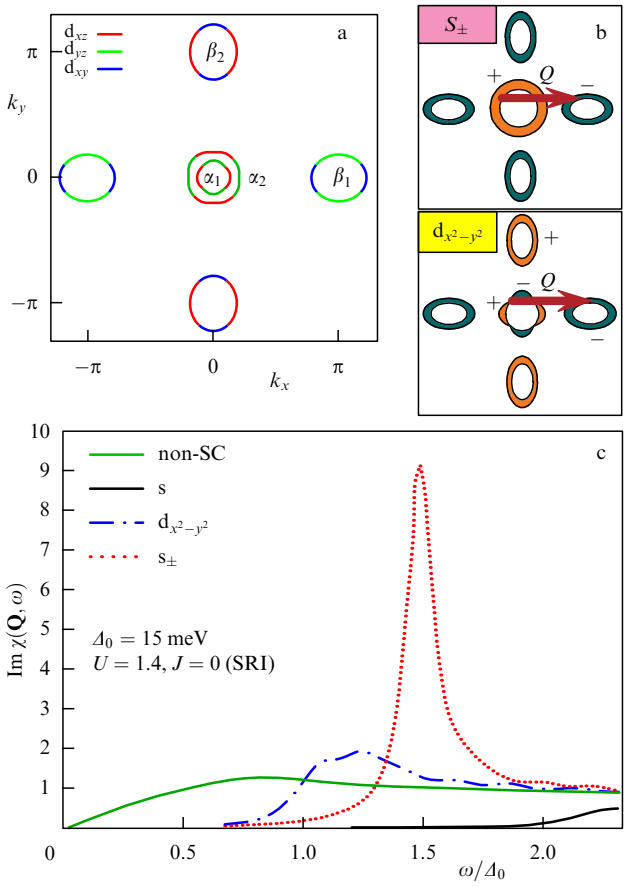

Figure 1. (Color online) (a) Fermi surface in the model of Ref. [23] upon electron doping ($x = 0.05$) in the Brillouin zone corresponding to one Fe atom per unit cell. The orbitals making the maximum contributions to the Fermi surface are shown by different colors: d_{xz} by red; d_{yz} by green; d_{xy} by blue. (b) Schematic structure of $s_\pm$ and $d_{x^2-y^2}$ type superconducting gaps on the Fermi surface; vector $\mathbf{Q} = (\pi, 0)$ connects electron and hole pockets. (c) Frequency dependence of the susceptibility $\mathrm{Im}\,\chi(\mathbf{q} = \mathbf{Q}, \omega)$ in the normal state (non-SC) and in the superconducting state with the symmetries s (s_{++}), $d_{x^2-y^2}$, and $s_\pm$. The calculation was done for Hubbard interaction $U = 1.4$ eV and Hund's exchange $J = 0$ in the presence of spin-rotational invariance (SRI). For the $s_\pm$ state, a resonance peak arises for $\omega < 2\Delta_0$.

density wave (SDW) order because of the nesting between the hole and electron Fermi surfaces with the wave vector $\mathbf{Q} = (\pi, 0)$ or $\mathbf{Q} = (0, \pi)$. With increasing doping x, the long-range SDW order disappears. In the case of electron doping, the hole pockets disappear when x exceeds some particular value, and only electron pockets are retained, as, e.g., in the case of $K_xFe_{2-y}Se_2$ and FeSe monolayers [4]. With increasing hole concentration, a new hole pocket first takes place around the point (π, π), and then the electron Fermi surfaces disappear. This situation arises, in particular, in KFe_2As_2. The fact that the maximum contributions to the band lying on the Fermi surface come from the $d_{xz,yz}$- and d_{xy}-orbitals is confirmed by the ARPES spectra [25, 26]. In this case, as will be shown below, the existence of several electron pockets and the multiorbital character of the bands substantially affect the superconducting pairing.

Before moving to the description of the multiorbital variant of the theory, let us describe how the spin-fluctuation theory of pairing is constructed in the single-band case with a Hubbard interaction Hamiltonian $H = \sum_f U n_{f\uparrow} n_{f\downarrow}$, where U is the single-site Coulomb (Hubbard) repulsion, and $n_{f\sigma}$ is the operator of the number of particles on the site f with a spin σ. The superconducting interaction in the singlet channel is governed by the Cooper vertex $\Gamma_{\uparrow\downarrow}$, which, in the spirit of the Berk–Schrieffer theory [27–29], is given by a diagrammatic series in the random-phase approximation (RPA) (Fig. 2). The basic element in this case is an electron–hole loop, i.e., the 'bare' susceptibility

$$\chi_0(\mathbf{q}, \mathrm{i}\omega_n) = \sum_{\mathbf{p}} \frac{f(\varepsilon_{\mathbf{p}+\mathbf{q}}) - f(\varepsilon_{\mathbf{p}})}{\mathrm{i}\omega_n - \varepsilon_{\mathbf{p}+\mathbf{q}} + \varepsilon_{\mathbf{p}}} ,$$

where $f(\varepsilon_{\mathbf{p}})$ is the Fermi distribution function for the electron dispersion $\varepsilon_{\mathbf{p}}$, and ω_n is the Matsubara frequency. The sum of loops and ladders yields

$$\begin{aligned} \Gamma_{\uparrow\downarrow} &= U(1 + U^2\chi_0^2 + \ldots) + U^2\chi_0(1 + U\chi_0 + \ldots) \\ &= \frac{U}{1 - U^2\chi_0^2} + \frac{U^2\chi_0}{1 - U\chi_0} \qquad (1) \\ &= \frac{3}{2} U^2\chi_{\mathrm{s}} - \frac{1}{2} U^2\chi_{\mathrm{c}} + U , \qquad (2) \end{aligned}$$

where χ_{s} and χ_{c} are the spin and charge susceptibilities, respectively:

$$\chi_{\mathrm{s,c}} = \frac{\chi_0}{1 \mp U\chi_0} . \qquad (3)$$

A magnetic instability develops in the system if the Stoner criterion is fulfilled: $1 = U\chi_0(\mathbf{q}, \omega = 0)$. The ferromagnetic instability corresponds to $\mathbf{q} = 0$; the AFM instability, which is of interest for us, arises at the antiferromagnetic wave vector $\mathbf{q} = \mathbf{Q}$. If we can avoid the development of the instability, for example, via doping, then no long-range order will appear, but the product $U\chi_0(\mathbf{q}, \omega = 0)$ will be close to unity, thus leading to a large magnitude of the spin susceptibility χ_{s} and, correspondingly, to its very large contribution to the Cooper vertex $\Gamma_{\uparrow\downarrow}$. However, unlike the electron–phonon interaction in the Bardeen–Cooper–Schrieffer (BCS) theory, $\Gamma_{\uparrow\downarrow}$ gives rise to effective repulsion interaction $V(\mathbf{k}, \mathbf{k}')$ rather than to attraction. If we write the Hamiltonian of the system in terms of the mean-field theory, explicitly separating the superconducting interaction

$$H = \sum_{\mathbf{k},\sigma} \varepsilon_{\mathbf{k}} a^{\dagger}_{\mathbf{k}\sigma} a_{\mathbf{k}\sigma} + \frac{1}{2} \sum_{\mathbf{k},\mathbf{k}',\sigma} V(\mathbf{k} - \mathbf{k}')\, a^{\dagger}_{-\mathbf{k}\sigma} a^{\dagger}_{\mathbf{k}\bar{\sigma}} a_{\mathbf{k}'\sigma} a_{\mathbf{k}'\bar{\sigma}} ,$$

where $\bar{\sigma} = -\sigma$ and $a^{\dagger}_{\mathbf{k}\sigma}$ is the creation operator of an electron with a momentum $\mathbf{k}$ and spin σ, then the equation for the gap will be as follows:

$$\Delta_{\mathbf{k}}(T) = -\sum_{\mathbf{k}'} \frac{V(\mathbf{k} - \mathbf{k}')}{2E_{\mathbf{k}'}} \Delta_{\mathbf{k}'}(T) \tanh \frac{E_{\mathbf{k}'}}{2T} , \qquad (4)$$

where $E_{\mathbf{k}} = \sqrt{\varepsilon_{\mathbf{k}}^2 + \Delta_{\mathbf{k}}^2}$. In the case of electron–phonon interaction with a coupling constant $g_{\mathrm{e-ph}}$, in the BCS theory we have $V(\mathbf{k} - \mathbf{k}') = -g^2_{\mathrm{e-ph}}$, and equation (4) has the solution $\Delta_{\mathbf{k}} = \Delta_0(T)$, which corresponds to the s type of superconducting order parameter. In iron compounds, the orbital fluctuations enhanced by electron–phonon interaction can lead to a sign-constant solution, which in the multiband case is called the s_{++} state [30, 31]. On the other hand, for the spin-fluctuation interaction we have $V(\mathbf{k} - \mathbf{k}') > 0$, and the s type of solution does not satisfy equation (4). In the case of spin fluctuations, $V(\mathbf{k} - \mathbf{k}')$ has a maximum at the wave vector $\mathbf{Q}$, and if we employ a very rough approximation, $V(\mathbf{k} - \mathbf{k}') = |\lambda|\delta(\mathbf{k} - \mathbf{k}' + \mathbf{Q})$, then equation (4) will take the form

$$\Delta_{\mathbf{k}}(T) = -|\lambda| \frac{\Delta_{\mathbf{k}+\mathbf{Q}}(T)}{2E_{\mathbf{k}+\mathbf{Q}}} \tanh \frac{E_{\mathbf{k}+\mathbf{Q}}}{2T} . \qquad (5)$$

It is obvious that the last equation has a solution if $\Delta_{\mathbf{k}}$ and $\Delta_{\mathbf{k}+\mathbf{Q}}$ have different signs. In the simplest case of $\Delta_{\mathbf{k}} = -\Delta_{\mathbf{k}+\mathbf{Q}}$ the equation acquires the form

$$1 = |\lambda| \frac{1}{2\,E_{\mathbf{k}+\mathbf{Q}}} \tanh \frac{E_{\mathbf{k}+\mathbf{Q}}}{2T} .$$

The solution defines a gap, which reverses sign at the vector $\mathbf{Q}$. If this vector connects different bands of the quasiparticles (Fermi surfaces belonging to different bands), which is realized, in particular, in iron compounds, then the solution of this type with an A_{1g} symmetry is called the $s_{\pm}$ state [22]. The competing states will be those with a B_{1g} and a B_{2g} symmetries, namely, those that have the d_{xy} and $d_{x^2-y^2}$ types of order parameter.

In the multiorbital case, the central subject of the spin-fluctuation theory — the dynamic spin susceptibility — is a tensor with respect to the orbital indices l, l', m, and m':

$$\chi^{ll',mm'}_{ss'}(\mathbf{q}, \mathrm{i}\Omega) = -\int_0^{\beta} \mathrm{d}\tau \exp(\mathrm{i}\Omega\tau) \left\langle T\tau S^s_{ll'}(\mathbf{q}, \tau)\, S^{s'}_{m'm}(-\mathbf{q}, 0) \right\rangle . \qquad (6)$$

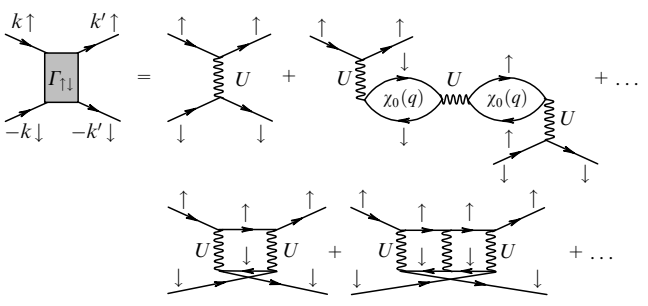

Figure 2. Cooper vertex $\Gamma_{\uparrow\downarrow}$ for a singlet superconducting state in the RPA.

Here, Ω is the Matsubara frequency; $S^s_{ll'}(\mathbf{q},\tau)$ is the sth component of the vector of the spin operator with the Matsubara time τ:

$$\mathbf{S}_{ll'}(\mathbf{q},\tau)=\frac{1}{2}\sum_{\mathbf{p},\alpha,\alpha'} a^{\dagger}_{\mathbf{p}l\alpha}(\tau)\,\hat{\boldsymbol{\sigma}}_{\alpha\alpha'}a_{\mathbf{p}+\mathbf{q}l'\alpha'}(\tau)\,,$$

where $\hat{\boldsymbol{\sigma}}$ is a vector composed of Pauli matrices $\hat{\sigma}$, and $a^{\dagger}_{\mathbf{p}l\alpha}$ is the operator of creation of an electron on the orbital l with a momentum $\mathbf{p}$ and spin α. To obtain a zero's order approximation, we decouple expression (6) via Wick's theorem, introduce normal and anomalous Green's functions

$$G_{ml\sigma\sigma'}(\mathbf{k},\tau)=-\left\langle T_\tau a_{\mathbf{k}m\sigma}(\tau)\,a^{\dagger}_{\mathbf{k}l\sigma'}(0)\right\rangle,$$

$$F^{\dagger}_{ml\sigma\sigma'}(\mathbf{k},\tau)=\left\langle T_\tau a^{\dagger}_{\mathbf{k}m\sigma}(\tau)\,a^{\dagger}_{-\mathbf{k}l\bar{\sigma}'}(0)\right\rangle,$$

$$F_{ml\sigma\sigma'}(\mathbf{k},\tau)=\left\langle T_\tau a_{\mathbf{k}m\sigma}(\tau)\,a_{-\mathbf{k}l\bar{\sigma}'}(0)\right\rangle,$$

transform to the Matsubara frequencies ω_n, and arrive at the following expression for the $(+-)$ component of the susceptibility in the absence of spin–orbit interaction:

$$\chi^{ll',mm'}_{0,+-}(\mathbf{q},\mathrm{i}\Omega)=-T\sum_{\omega_n,\mathbf{p}}\left[G_{ml\uparrow\uparrow}(\mathbf{p},\mathrm{i}\omega_n)\,G_{l'm'\downarrow\downarrow}(\mathbf{p}+\mathbf{q},\mathrm{i}\Omega+\mathrm{i}\omega_n)\right.$$
$$\left.-F^{\dagger}_{lm'\uparrow\downarrow}(\mathbf{p},-\mathrm{i}\omega_n)\,F_{l'm\downarrow\uparrow}(\mathbf{p}+\mathbf{q},\mathrm{i}\Omega+\mathrm{i}\omega_n)\right]. \qquad (7)$$

The physical (observed) susceptibility is obtained at the coincident orbital indices of the two Green's functions entering into the vertex, i.e., at $l'=l$ and $m'=m$: $\chi_{+-}(\mathbf{q},\mathrm{i}\Omega)=(1/2)\sum_{l,m}\chi^{ll,mm}_{+-}(\mathbf{q},\mathrm{i}\Omega)$.

The Cooper vertex $\Gamma_{\uparrow\downarrow}$ has to be calculated in the normal phase, where there are no anomalous Green's functions. The Green's functions in the orbital basis are off-diagonal and depend on two orbital indices. It makes sense to move to the band basis constructed using operators of electron creation and annihilation, $b^{\dagger}_{\mathbf{k}\mu\sigma}$ and $b_{\mathbf{k}\mu\sigma}$, with the band index μ, where the Green's functions are diagonal: $G_{\mu\sigma}(\mathbf{k},\mathrm{i}\Omega)=1/(\mathrm{i}\Omega-\varepsilon_{\mathbf{k}\mu\sigma})$. The transition from the orbital to band basis is implemented with the aid of the matrix elements $\varphi^{\mu}_{\mathbf{k}m}$: $|\sigma m\mathbf{k}\rangle=\sum_\mu\varphi^{\mu}_{\mathbf{k}m}|\sigma\mu\mathbf{k}\rangle$. In this case, $a_{\mathbf{k}m\sigma}=\sum_\mu\varphi^{\mu}_{\mathbf{k}m}b_{\mathbf{k}\mu\sigma}$, and the susceptibility takes the form

$$\chi^{ll',mm'}_{0,+-}(\mathbf{q},\mathrm{i}\Omega)=-T\sum_{\omega_n,\mathbf{p},\mu,\nu}\varphi^{\mu}_{\mathbf{p}m}\varphi^{*\mu}_{\mathbf{p}l}G_{\mu\uparrow}(\mathbf{p},\mathrm{i}\omega_n)$$
$$\times\,G_{\nu\downarrow}(\mathbf{p}+\mathbf{q},\mathrm{i}\Omega+\mathrm{i}\omega_n)\,\varphi^{\nu}_{\mathbf{p}+\mathbf{q}l'}\varphi^{*\nu}_{\mathbf{p}+\mathbf{q}m'}\,. \qquad (8)$$

Below, we will rely on the model of the band structure H_0 borrowed from paper [23], which is based on DFT calculations [24] for a single-layer LaFeAsO pnictide. As the interaction, we will use the two-particle Hamiltonian with a single-site interaction of the general form [23, 32–34]:

$$H=H_0+U\sum_{f,m}n_{fm\uparrow}n_{fm\downarrow}+U'\sum_{f,m<l}n_{fl}\,n_{fm}$$
$$+J\sum_{f,m<l}\sum_{\sigma,\sigma'}a^{\dagger}_{fl\sigma}a^{\dagger}_{fm\sigma'}a_{fl\sigma'}a_{fm\sigma}+J'\sum_{f,m\neq l}a^{\dagger}_{fl\uparrow}a^{\dagger}_{fl\downarrow}a_{fm\downarrow}a_{fm\uparrow}\,, \qquad (9)$$

where $n_{fm}=n_{fm\uparrow}+n_{fm\downarrow}$, f is the index of the site; U and U' are the intra- and interorbital Hubbard repulsions; J is Hund's exchange, and J' is the pair hopping. The parameters usually preserve spin-rotation invariance, which leads to a decrease in the number of free parameters of the theory because of the relationships $U'=U-2J$ and $J'=J$.

Based on the interaction involved in Hamiltonian (9), we can construct an RPA for the spin susceptibility $\chi_{+-}(\mathbf{q},\mathrm{i}\Omega)$ [23]. To obtain the solution, we transform from tensors to matrices with the indices $i=l+l'n_{\mathrm{orb}}$ and $j=m+m'n_{\mathrm{orb}}$, where n_{orb} is the number of orbitals. Then, in the matrix form, the spin susceptibility in the RPA is written down as

$$\hat{\chi}_{+-}=(\hat{1}-\hat{\chi}_{0,+-}\hat{U}^{+-})^{-1}\,\chi_{0,+-}\,, \qquad (10)$$

where $\hat{U}^{+-}$ is the matrix of interactions in the $(+-)$ channel.

The Cooper vertex in the multiorbital case is similar to that in the single-band case (1):

$$\Gamma^{l_1l_2l_3l_4}_{\uparrow\downarrow}(\mathbf{k},\mathbf{k}',\omega)=\left[\frac{3}{2}\,\hat{U}_{\mathrm{s}}\hat{\chi}_{\mathrm{s}}(\mathbf{k}-\mathbf{k}',\omega)\,\hat{U}_{\mathrm{s}}\right.$$
$$\left.-\frac{1}{2}\,\hat{U}_{\mathrm{c}}\hat{\chi}_{\mathrm{c}}(\mathbf{k}-\mathbf{k}',\omega)\,\hat{U}_{\mathrm{c}}+\frac{1}{2}\,\hat{U}_{\mathrm{s}}+\frac{1}{2}\,\hat{U}_{\mathrm{c}}\right]_{l_1l_2l_3l_4}, \qquad (11)$$

where $\hat{\chi}_{\mathrm{s,c}}=(\hat{1}\mp\hat{\chi}_0\hat{U}_{\mathrm{s,c}})^{-1}\hat{\chi}_0$ is the spin (s) and charge (c) susceptibilities, $\hat{U}_{\mathrm{s,c}}$ are the matrices of interaction in the spin and charge channels, and l_1 to l_4 are the orbital indices.

The necessity of constructing the theory in orbital representation stems from the fact that just in this representation the Hubbard interaction (9) remains local. The superconducting pairs, however, are formed at the level of bands rather than orbitals; therefore, we should transform the Cooper vertex into a band basis utilizing matrix elements $\varphi^{\mu}_{\mathbf{k}m}$:

$$\Gamma^{\mu\nu}(\mathbf{k},\mathbf{k}',\omega)=\sum_{l_1,l_2,l_3,l_4}\varphi^{*\mu}_{\mathbf{k}l_2}\varphi^{*\mu}_{-\mathbf{k}l_3}\Gamma^{l_1l_2l_3l_4}_{\uparrow\downarrow}(\mathbf{k},\mathbf{k}',\omega)\,\varphi^{\nu}_{\mathbf{k}'l_1}\varphi^{\nu}_{-\mathbf{k}'l_4}. \qquad (12)$$

Calculations show that $\Gamma^{\mu\nu}$ rapidly decreases with increasing frequency in the range of frequencies that are much lower than the band width. Although the equation for the superconducting gap depends, generally speaking, on $\mathrm{Im}\,\Gamma^{\mu\nu}$, the momenta $\mathbf{k}$ and $\mathbf{k}'$ making the main contribution to the pairing should correspond to the small frequencies at which these momenta lie near the Fermi surface. Similarly to the case where the coupling constant for the electron–phonon interaction is determined by the integral of the Eliashberg function $\alpha^2F(\omega)$ taken with respect to frequency, here, using the Kramers–Kronig relationship, we obtain

$$\int_0^{\infty}\mathrm{d}\omega\,\frac{\mathrm{Im}\,\Gamma^{\mu\nu}(\mathbf{k},\mathbf{k}',\omega)}{\omega}=\mathrm{Re}\,\Gamma^{\mu\nu}(\mathbf{k},\mathbf{k}',\omega=0)\equiv\tilde{\Gamma}^{\mu\nu}(\mathbf{k},\mathbf{k}')\,. \qquad (13)$$

Thus, the problem of the calculation of the effective pairing interaction reduces to finding the real part of $\Gamma^{\mu\nu}$ at the zero frequency, which substantially simplifies the calculation procedure.

If we represent the order parameter $\Delta_{\mathbf{k}}$ in the form of a product of the amplitude Δ_0 by the angular part $g_{\mathbf{k}}$, we can determine the dimensionless coupling parameter λ as a result of the solution to the problem for the eigenvalues (λ) and eigenvectors ($g_{\mathbf{k}}$) [23]:

$$\lambda g_{\mathbf{k}}=-\sum_\nu\oint_\nu\frac{\mathrm{d}\mathbf{k}'_{\parallel}}{2\pi}\,\frac{1}{2\pi v_{\mathbf{F}\mathbf{k}'}}\,\tilde{\Gamma}^{\mu\nu}(\mathbf{k},\mathbf{k}')\,g_{\mathbf{k}'}\,, \qquad (14)$$

where $v_{\mathbf{F}\mathbf{k}}$ is the Fermi velocity, the contour integral is taken over $\mathbf{k}'_{\parallel}$ belonging to the νth Fermi surface, and the band index μ is unambiguously determined by the fact which of the Fermi surfaces the momentum $\mathbf{k}$ belongs to. The positive λ

correspond to attraction; their maximum corresponds to the maximum value of T_c, i.e., the most favorable symmetry of the pairing and the gap function, which is determined by $g_{\mathbf{k}}$. By aligning λ according to decreasing values, we can see what symmetries and gap structures are most favorable and which will be competing among themselves.

From the viewpoint of the mechanism of superconducting pairing, both the spin-fluctuation theories [23, 34, 35] with their self-consistent generalizations in the fluctuation-exchange (FLEX) approximation [36–38] and the renormalization group analysis [39, 40] are quite complicated numerical methods. But since, in the case of pairing, it is the amplitude of scattering in the particle–particle channel on the Fermi surface that is important, the angular dependence of this amplitude can be expanded in terms of the same harmonics as the $\Delta_{\mathbf{k}}$ is expanded. Such a method, which is called LAHA (lowest angular harmonics approximation), makes it possible to describe pairing in iron compounds both in the case of low doping and upon very strong doping with electrons or holes, using a limited set of parameters and without doing complex calculations [41–43]. The main assumption of the LAHA is the fact that the Cooper vertex $\tilde{\Gamma}^{\mu\nu}(\mathbf{k},\mathbf{k}')$ can be factorized in momenta $\mathbf{k}$ and $\mathbf{k}'$ as follows:

$$\tilde{\Gamma}^{\eta}(\mathbf{k},\mathbf{k}') = \sum_{m,n} C^{\eta}_{mn}\, \Psi^{\eta}_{m}(\mathbf{k})\, \Psi^{\eta}_{n}(\mathbf{k}')\,, \tag{15}$$

where the index η corresponds to the symmetry group of the order parameter, C^{η}_{mn} are some coefficients, and the function Ψ makes up the expansion in terms of angular harmonics. The expansions, depending on η, have different functional forms. Thus, for example, $\Psi^{A_{1g}}_{m}(\mathbf{k}) = a_m + b_m \cos(4\phi_{\mathbf{k}}) + c_m \cos(8\phi_{\mathbf{k}}) + \ldots$ for the A_{1g} representation, and for the B_{1g} representation one has $\Psi^{B_{1g}}_{m}(\mathbf{k}) = a^*_m \cos(2\phi_{\mathbf{k}}) + b^*_m \cos(6\phi_{\mathbf{k}}) + c^*_m \cos(10\phi_{\mathbf{k}}) + \ldots$.

Now, the problem can be reduced to finding a function $\tilde{\Gamma}^{\eta}_{ab}$, where a and b correspond to the numbers of the Fermi surfaces. Thus, in Fig. 1 these are hole ($\alpha_{1,2}$) and electron ($\beta_{1,2}$) pockets. For example, for the extended s- and $d_{x^2-y^2}$-components, we can write out the following expressions

$$\begin{aligned}
\tilde{\Gamma}_{\alpha_i\alpha_j} &= U_{\alpha_i\alpha_j} + \tilde{U}_{\alpha_i\alpha_j}\cos(2\phi_i)\cos(2\phi_j)\,,\\
\tilde{\Gamma}_{\alpha_i\beta_1} &= U_{\alpha_i\beta}\left[1 + 2\gamma_{\alpha_i\beta}\cos(2\theta_1)\right] + \tilde{U}_{\alpha_i\beta}\\
&\quad\times\left[1 + 2\tilde{\gamma}_{\alpha_i\beta}\cos(2\theta_1)\right]\cos(2\phi_i)\,,\\
\tilde{\Gamma}_{\beta_1\beta_1} &= U_{\beta\beta}\Big\{1 + 2\gamma_{\beta\beta}\left[\cos(2\theta_1) + \cos(2\theta_2)\right]\\
&\quad + 4\gamma'_{\beta\beta}\cos(2\theta_1)\cos(2\theta_2)\Big\}\\
&\quad + \tilde{U}_{\beta\beta}\Big\{1 + 2\tilde{\gamma}_{\beta\beta}\left[\cos(2\theta_1) + \cos(2\theta_2)\right]\\
&\quad + 4\tilde{\gamma}'_{\beta\beta}\cos(2\theta_1)\cos(2\theta_2)\Big\}\,,
\end{aligned}$$

where U_{ij} and $\tilde{U}_{ij}$ are the interactions in the s- and d-channels, respectively; $\gamma_{\alpha_i\beta}$, $\gamma_{\beta\beta}$, $\gamma'_{\beta\beta}$, $\tilde{\gamma}_{\alpha_i\beta}$, $\tilde{\gamma}'_{\beta\beta}$ determine the degree of interaction anisotropy, and ϕ_i and θ_i are the angles on the hole and electron Fermi surfaces counted from the k_x-axis. The equation for the order parameter is reduced here to the matrix equation 4×4, which can easily be solved. The coefficients C^{η}_{mn} and all a, b, etc. entering the expansion in Ψ can be obtained from a comparison with the calculation of the total $\tilde{\Gamma}^{\mu\nu}(\mathbf{k},\mathbf{k}')$ using Eqns (11) and (12). A comparison of the results for the order parameters has shown that the LAHA reproduces the RPA results quite well [42].

One of the advantages of the LAHA consists in the possibility of varying the effective interaction parameters U_{ij} and $\tilde{U}_{ij}$, determining thereby to which extent this or that concrete solution for the gap is stable. In this fermiological picture, one can clearly distinguish which of the interactions leads to pairing.

Figure 3 schematically depicts a phase diagram and the Fermi surfaces for various levels of doping. Depending on the topology and relative volumes of the hole and electron pockets, a competition can arise between the gaps of the $s_{\pm}$

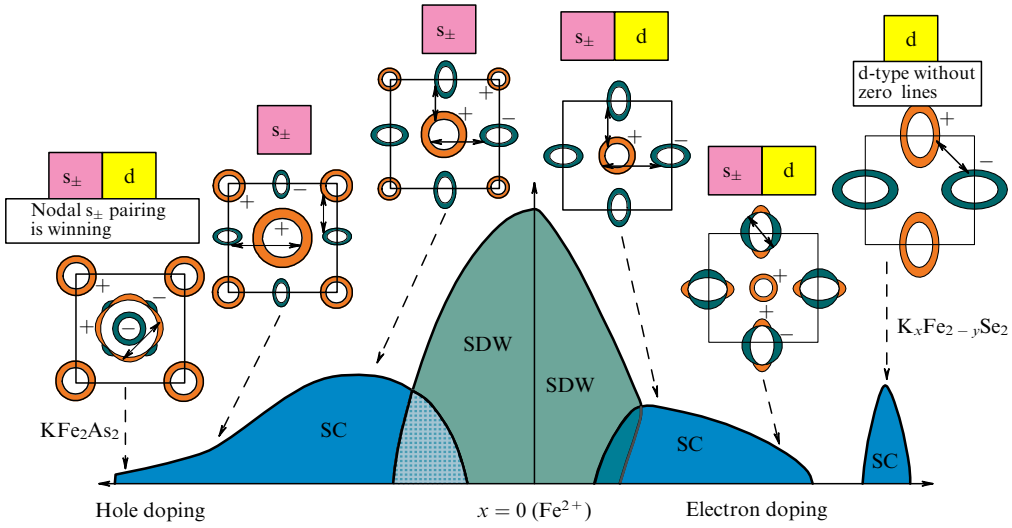

Figure 3. (Color online). Schematic phase diagram of iron compounds for both hole and electron dopings. The coexistence of AFM (SDW) and superconducting (SC) phases appears on a microscopic level for the case of electron doping, and on the macroscopic level (division into SDW and SC domains) upon hole doping. The qualitative picture of the symmetries of the superconducting parameter that follows from the spin-fluctuation theory [16, 23, 35] and from the LAHA [42, 43] for the two-dimensional system is shown on symmetrical Fermi surfaces in the insets above the phase diagram; $s_{\pm}$ and d stand for the predominant and subdominant symmetries of pairing. Solid lines with an arrow at both ends (↔) indicate the predominant interaction.

and d types. However, it is the $s_{\pm}$ state that always wins in the presence of both electron and hole pockets. The predominant interactions U_{ij} and $\tilde{U}_{ij}$ that were obtained from the analysis of the LAHA results are shown by arrows connecting the particles on the Fermi surfaces. Thus, the strongest interaction $U_{\alpha_i\beta}$ in the case of low doping is between the electron and hole pockets, and the dominating state has the $s_{\pm}$-symmetry. Upon electron doping, the repulsion $U_{\beta\beta}$ inside the electron pocket is large, and it is best for the system to form a sign-reversed gap on the electron pockets in order to reduce this contribution. In this case, an $s_{\pm}$-state has nodal lines at electron Fermi surfaces. If the electron doping is very high (as in $K_xFe_{2-y}Se_2$), when the hole pockets disappear, the system forms d-type superconductivity because of the strong interaction between the electron Fermi pockets. One question remains open: whether or not such a state would be favorable as compared to the bonding–antibonding $s_{\pm}$-state [16, 44] upon the transformation to the Brillouin zone corresponding to two Fe atoms per unit cell. It seems that, because the spin–orbit interaction is present in this case [45], and because of the following from it hybridization along the symmetry directions, the bonding–antibonding $s_{\pm}$-state should be most advantageous [46]. However, as follows from the calculations in the 10-orbital model for $K_{0.8}Fe_{1.7}Se_2$ and $K_{0.85}Fe_{1.8}Se_2$, it is the pairing of the $d_{x^2-y^2}$ type that always dominates [47].

For the hole doping, on the contrary, the appearance of a new hole pocket γ near the point (π, π) leads to the stabilization of an $s_{\pm}$-state without nodes on the Fermi surface. This picture is affected by the orbital character of the bands. Since the pocket γ is mainly formed by the d_{xy} orbital, as are the small regions on the electron pockets (see Fig. 1), the new channel of scattering of this pocket by the electron pockets leads to the 'isotropization' of the gap on electron pockets. With a further doping by holes, when the electron pockets disappear, as in KFe_2As_2, the strong interaction inside the hole pocket α_2 forces the system to form a sign-reversed gap with nodes on this pocket. The symmetry of the gap refers, as before, to the A_{1g} representation and corresponds to the $s_{\pm}$-state with added higher angular harmonics [43].

As to the experimental observation of the $s_{\pm}$-state, the first results were obtained using inelastic neutron scattering. Since $\chi_0(\mathbf{q}, \omega)$ describes the particle–hole excitations and since all excitations at frequencies less than $\approx 2\Delta_0$ (at $T = 0$) are absent in the superconducting state, the imaginary part $\operatorname{Im}\chi_0(\mathbf{q}, \omega)$ becomes finite only above this frequency value. The anomalous Green's functions entering Eqn (7) give rise to terms proportional to $1 - \Delta_{\mathbf{k}}\Delta_{\mathbf{k}+\mathbf{q}}/E_{\mathbf{k}}E_{\mathbf{k}+\mathbf{q}}$. These are the so-called *anomalous coherence factors*. At the Fermi level, one has $E_{\mathbf{k}} \equiv (\varepsilon_{\mathbf{k}}^2 + \Delta_{\mathbf{k}}^2)^{1/2} = |\Delta_{\mathbf{k}}|$. If $\Delta_{\mathbf{k}}$ and $\Delta_{\mathbf{k}+\mathbf{q}}$ have the same sign, the coherence factors will be equal to zero, which will lead to a gradual increase in the spin susceptibility with increasing frequency in the range $\omega > \Omega_c$, where $\Omega_c = \min(|\Delta_{\mathbf{k}}| + |\Delta_{\mathbf{k}+\mathbf{q}}|)$, whereas at frequencies lower than Ω_c, we obtain $\operatorname{Im}\chi_0(\mathbf{q}, \omega) = 0$. This can be seen from Fig. 1 for superconductivity of the classical s type (s_{++}-state). If, however, as in the case of $s_{\pm}$- and d-states in iron compounds, the vector $\mathbf{q} = \mathbf{Q} = (\pi, 0)$ connects the Fermi surfaces with different signs of the gap ($\operatorname{sgn}\Delta_{\mathbf{k}} \neq \operatorname{sgn}\Delta_{\mathbf{k}+\mathbf{q}}$), then the coherence factors are nonzero and a jump appears in the imaginary part of χ_0 at $\omega = \Omega_c$. In accordance with the Kramers–Kronig relations, a logarithmic singularity appears in the real part of susceptibility. For a certain set of parameters U, U', J, J' entering into the matrix $\hat{U}^{\pm}$, the nonzero value of $\operatorname{Re}\chi_0$ and $\operatorname{Im}\chi_0 = 0$ lead to a divergence of the imaginary part of the susceptibility (10) in the RPA. The corresponding peak in $\operatorname{Im}\chi(\mathbf{Q}, \omega)$, which is called the 'spin resonance,' appears for the frequencies $\Omega_{\text{res}} \leqslant \Omega_c$. This peak is quite pronounced for the $s_{\pm}$-state in Fig. 1. In the $d_{x^2-y^2}$-symmetry case (although, in principle, the resonance could arise because of the sign-reversed character of the gap), the vector $\mathbf{Q}$ connects the states on the hole Fermi surface near the nodes of the gap $\Delta_{\mathbf{k}}$, and the total gap in $\operatorname{Im}\chi_0$, which is determined by Ω_c, is very low. Since $\Omega_c \ll \Delta_0$, the jump in $\operatorname{Im}\chi_0$ is negligibly small, and the susceptibility in the RPA shows a slight increase in comparison with that for the normal state (see Fig. 1). The same is valid for d_{xy}- and $d_{x^2-y^2} + id_{xy}$-symmetries [48] and for the triplet p-type pairing [49].

Thus, the existence of a spin resonance refers to an exclusive property of the $s_{\pm}$-state. For iron compounds, the spin resonance was predicted theoretically [48, 49] and then revealed experimentally in the 1111, 122, and 11 families of pnictides and chalcogenides [50–58].

By introducing an additional damping of quasiparticles and by adjusting parameters, we can attain the appearance of a peak in the magnetic susceptibility in the s_{++}-state at frequencies above Ω_c [59, 60]. From the experimental viewpoint, it is important to distinguish the situation with appearing a resonance peak for $\Omega_{\text{res}} \leqslant \Omega_c$ from that with the enhanced susceptibility for $\omega > \Omega_c$. The first case refers to the $s_{\pm}$-state and indirectly confirms the spin-fluctuation mechanism of the superconductivity; the second case corresponds to the s_{++}-state and to the theory of superconductivity due to orbital fluctuations or electron–phonon interaction. No exact answer exists so far as to which of them is correct, but the present body of experimental data on both the spin resonance and on the quasiparticle interference scattering, penetration depth, heat capacity, and many other observed characteristics indicates in favor of the $s_{\pm}$-state with a sign reversal [16].

Summarizing, we conclude that, in spite of the variety of the materials, the multiorbital spin-fluctuation theory of pairing can explain many observed features of iron-based superconductors, in particular, the different variants of the experimentally examined behaviors of the superconducting gap. The anisotropic $s_{\pm}$-state and its nodal structure on Fermi surfaces are quite sensitive to some details of the electronic structure, such as the orbital character of the bands, spin–orbit interaction, and changes in the band structure due to the doping.

Acknowledgments

I am very grateful to O V Dolgov, I M Eremin, A Kordyuk, I I Mazin, V M Pudalov, M V Sadovskii, Yu M Togushova, P J Hirschfield, and A V Chubukov for the fruitful discussions. This work was supported in part by the Russian Foundation for Basic Research (project No. 13-02-01395), by the Program No. 20.7 of the Presidium of the Russian Academy of Sciences, by the 'President Grant for Government Support of the Leading Scientific Schools of the Russian Federation' (No. NSh-2886.2014.2), by the Dinastiya Foundation and the International Center for Fundamental Physics in Moscow.

References

1. Kamihara Y et al. *J. Am. Chem. Soc.* **130** 3296 (2008)
2. Fujioka M et al., arXiv:1401.5611

3. Wang Q-Y et al. *Chinese Phys. Lett.* **29** 037402 (2012)
4. Liu D et al. *Nature Commun.* **3** 931 (2012)
5. Sadovskii M V *Phys. Usp.* **51** 1201 (2008); *Usp. Fiz. Nauk* **178** 1243 (2008)
6. Ivanovskii A L *Phys. Usp.* **51** 1229 (2008); *Usp. Fiz. Nauk* **178** 1273 (2008)
7. Izyumov Yu A, Kurmaev E Z *Phys. Usp.* **51** 1261 (2008); *Usp. Fiz. Nauk* **178** 1307 (2008)
8. Ishida K, Nakai Y, Hosono H *J. Phys. Soc. Jpn.* **78** 062001 (2009)
9. Johnston D C *Adv. Phys.* **59** 803 (2010)
10. Paglione J, Greene R L *Nature Phys.* **6** 645 (2010)
11. Mazin I I *Nature* **464** 183 (2010)
12. Lumsden M D, Christianson A D *J. Phys. Condens. Matter* **22** 203203 (2010)
13. Wen H-H, Li S *Annu. Rev. Condens. Matter Phys.* **2** 121 (2011)
14. Basov D N, Chubukov A V *Nature Phys.* **7** 272 (2011)
15. Stewart G R *Rev. Mod. Phys.* **83** 1589 (2011)
16. Hirschfeld P J, Korshunov M M, Mazin I I *Rep. Prog. Phys.* **74** 124508 (2011)
17. Boeri L, Dolgov O V, Golubov A A *Phys. Rev. Lett.* **101** 026403 (2008)
18. Eschrig H, arXiv:0804.0186
19. Ning F et al. *J. Phys. Soc. Jpn.* **78** 013711 (2009)
20. Lebègue S *Phys. Rev. B* **75** 035110 (2007)
21. Singh D J, Du M-H *Phys. Rev. Lett.* **100** 237003 (2008)
22. Mazin I I et al. *Phys. Rev. Lett.* **101** 057003 (2008)
23. Graser S et al. *New J. Phys.* **11** 025016 (2009)
24. Cao C, Hirschfeld P J, Cheng H-P *Phys. Rev. B* **77** 220506(R) (2008)
25. Kordyuk A A *Low Temp. Phys.* **38** 888 (2012); *Fiz. Nizk. Temp.* **238** 1119 (2012)
26. Brouet V et al. *Phys. Rev. B* **86** 075123 (2012)
27. Berk N F, Schrieffer J R *Phys. Rev. Lett.* **17** 433 (1966)
28. Scalapino D J *J. Low Temp. Phys.* **117** 179 (1999)
29. Scalapino D J, Loh E (Jr.), Hirsch J E *Phys. Rev. B* **34** 8190(R) (1986)
30. Kontani H, Onari S *Phys. Rev. Lett.* **104** 157001 (2010)
31. Onari S, Kontani H *Phys. Rev. B* **85** 134507 (2012)
32. Castellani C, Natoli C R, Ranninger J *Phys. Rev. B* **18** 4945 (1978)
33. Oleś A M *Phys. Rev. B* **28** 327 (1983)
34. Kuroki K et al. *Phys. Rev. Lett.* **101** 087004 (2008)
35. Kemper A F et al. *New J. Phys.* **12** 073030 (2010)
36. Ikeda H *J. Phys. Soc. Jpn.* **77** 123707 (2008)
37. Ikeda H, Arita R, Kuneš J *Phys. Rev. B* **81** 054502 (2010)
38. Zhang J et al. *Phys. Rev. B* **79** 220502(R) (2009)
39. Chubukov A V, Efremov D V, Eremin I *Phys. Rev. B* **78** 134512 (2008)
40. Thomale R et al. *Phys. Rev. Lett.* **106** 187003 (2011)
41. Maiti S et al. *Phys. Rev. Lett.* **107** 147002 (2011)
42. Maiti S et al. *Phys. Rev. B* **84** 224505 (2011)
43. Maiti S, Korshunov M M, Chubukov A V *Phys. Rev. B* **85** 014511 (2012)
44. Mazin I I *Phys. Rev. B* **84** 024529 (2011)
45. Korshunov M M et al. *J. Supercond. Novel Magn.* **26** 2873 (2013)
46. Khodas M, Chubukov A V *Phys. Rev. Lett.* **108** 247003 (2012)
47. Kreisel A et al. *Phys. Rev. B* **88** 094522 (2013)
48. Korshunov M M, Eremin I *Phys. Rev. B* **78** 140509(R) (2008)
49. Maier T A, Scalapino D J *Phys. Rev. B* **78** 020514(R) (2008)
50. Inosov D S et al. *Nature Phys.* **6** 178 (2010)
51. Christianson A D et al. *Nature* **456** 930 (2008)
52. Lumsden M D et al. *Phys. Rev. Lett.* **102** 107005 (2009)
53. Christianson A D et al. *Phys. Rev. Lett.* **103** 087002 (2009)
54. Park J T et al. *Phys. Rev. B* **82** 134503 (2010)
55. Argyriou D N et al. *Phys. Rev. B* **81** 220503(R) (2010)
56. Castellan J-P et al. *Phys. Rev. Lett.* **107** 177003 (2011)
57. Qiu Y et al. *Phys. Rev. Lett.* **103** 067008 (2009)
58. Babkevich P et al. *J. Phys. Condens. Matter* **22** 142202 (2010)
59. Onari S, Kontani H, Sato M *Phys. Rev. B* **81** 060504(R) (2010)
60. Onari S, Kontani H *Phys. Rev. B* **84** 144518 (2011)

PACS numbers: **74.25.–q**, **74.45.+c**, 74.62.Dh, 74.70.Xa
DOI: 10.3367/UFNe.0184.201408i.0888

Andreev spectroscopy of iron-based superconductors: temperature dependence of the order parameters and scaling of $\Delta_{L,S}$ with T_c

T E Kuzmicheva, S A Kuzmichev, M G Mikheev, Ya G Ponomarev, S N Tchesnokov, V M Pudalov, E P Khlybov, N D Zhigadlo

1. Introduction

The unexpected discovery in 2006 [1] of the first layered Fe-based high-temperature superconductor (HTSC), LnOFePn (where Ln is lanthanide, Pn is pnictide; hereafter referred to as 1111), becomes a key issue in modern solid-state physics. Since 2008, the class of iron-based superconductors has greatly expanded: several families of iron pnictides and chalcogenides have been synthesized [2–4]. The crystal structure of oxypnictides is reminiscent of that of cuprates and is, in fact, a stack of superconducting Fe–As layers alternating along the *c*-direction with spacers, nonsuperconducting oxide blocks, Ln–O. In spite of the pronounced layered structure and anisotropic physical properties, the electron subsystem in Fe-based superconductors is less quasi-two-dimensional than that in cuprate HTSC, because the height of the Fe–As blocks exceeds the thickness of the CuO_2 planes, whereas the distance between superconducting blocks in iron-based superconductors is significantly shorter than that in cuprates. This seems to be a reason [5] why the critical temperature of Fe-based superconductors, though being as high as $T_c \approx 57.5$ K [6], still does not reach the cuprate one.

Superconductivity in novel materials emerges with the suppression of a spin-density-wave ground state under doping of the superconducting Fe–As layers or under external pressure [7]. The key distinction from cuprates, however, lies in the multiband nature of newly discovered superconductivity in iron-based materials. Band structure calculations have shown (for a review, see Ref. [8]) the coexistence of the electron and the hole quasi-two-dimensional bands in these com-

T E Kuzmicheva. Lebedev Physical Institute, Russian Academy of Sciences, Moscow; Lomonosov Moscow State University, Faculty of Physics, Russian Federation
E-mail: kute@sci.lebedev.ru
S A Kuzmichev, M G Mikheev, Ya G Ponomarev, S N Tchesnokov. Lomonosov Moscow State University, Faculty of Physics Russian Federation
V M Pudalov. Lebedev Physical Institute, Russian Academy of Sciences, Moscow, Russian Federation; Moscow Institute of Physics and Technology (State University), Dolgoprudnyi, Moscow region, Russian Federation
E P Khlybov. Vereshchagin Institute of High Pressure Physics, Russian Academy of Sciences, Troitsk, Moscow region, Russian Federation; International Laboratory for High Magnetic Fields and Low Temperatures, Wroclaw, Poland
N D Zhigadlo. Laboratory for Solid State Physics, ETH Zurich, Zurich, Switzerland

Uspekhi Fizicheskikh Nauk **184** (8) 888 – 897 (2014)
DOI: 10.3367/UFNr.0184.201408i.0888
Translated by T E Kuzmicheva; edited by A Radzig